Waveform Design with Constellation Extension for OFDM Dual-Functional Radar-Communications

Ebubekir Memisoglu, Talha Yılmaz, and Hüseyin Arslan, *Fellow, IEEE*

***Abstract*—Orthogonal frequency division multiplexing (OFDM) is widely used and works efficiently for the communication, but emerging applications requires OFDM to be flexible to meet sensing requirements. The time-frequency waveform design of OFDM for dual-functional radar-communications (DFRC) is critical to achieve the future communication and sensing requirements. Therefore, we propose a novel method to minimize Cramér-Rao bounds (CRBs) of the delay and Doppler estimation to improve radar performance of an OFDM DFRC system. Although some methods are proposed in the literature to improve the CRBs, these methods either require feedforward signaling or subcarrier reservation. However, it is possible to exploit the constellation extension of quadrature amplitude modulation (QAM) to achieve lower CRBs without these requirements. Therefore, the proposed method provides a transparent communication along with the CRB minimization for conventional OFDM systems. For the evaluation of the proposed method, CRB and symbol error rate (SER) are considered in the simulation results. Furthermore, the theoretical SER analysis of the proposed method is derived to understand the effects of CRB minimization on the communication performance.**

***Index Terms*—OFDM, dual-function radar-communications, waveform design, constellation extension, QAM, power optimization, Cramér-Rao bound (CRB).**

I. Introduction

FAST development of wireless devices and new applications have drastically increased the wireless data traffic, and current wireless networks cannot comply with the upcoming challenges [1]. Thus, to satisfy the demanding requirements of the new services and applications, wireless communication systems had to extend their capabilities further into the frequency spectrum to access larger amounts of bandwidth [2]–[4]. The spectral expansion of wireless technologies has started to overlap with radar operating bands, causing a great spectrum scarcity [5]–[8]. Furthermore, various applications such as future cellular networks [9], vehicular networks [10], [11], and indoor mapping [12], [13] requires sensing capabilities as well as advanced wireless communication capabilities. Motivated by the reasons above joint radar-communications (JRC) research has gathered great attention. In particular, JRC research consists of two main perspectives; radar-communication coexistence (RCC) and dual-functional radar-communications (DFRC) [5]. RCC aims at developing efficient interference management techniques, so that the radar and communication systems can operate without unduly interfering with each other. On the other hand, DFRC techniques are focused on designing joint systems that can simultaneously perform wireless communication and remote sensing. While RCC approaches require sharing of information between radar and communication systems, or rely on existence of a control center with the coordination capability, DFRC approaches allow for easier cooperation, and decongest the RF environment by using the same signal for both radar and communication functionalities. The authors in [14]–[16] propose RCC systems utilizing orthogonal coexistence, non-orthogonal multiple access (NOMA), and multiple-input multiple-output (MIMO), respectively.

Due to orthogonal frequency division multiplexing (OFDM)'s great performance under frequency selective channels, robust synchronization [17], [18], and native MIMO support OFDM continues to be the cornerstone of current wireless communication standards. Nevertheless, as in conventional OFDM systems, high peak-to-average power ratio (PAPR) is one of the main drawbacks for the OFDM DFRC systems. However, various techniques are already developed to overcome this drawback, such as coding and tone reservation [19]–[21]. Since PAPR is shown to be manageable and OFDM's communication performance is coupled with high accuracy radar operation [22]–[24], OFDM is an excellent candidate as a DFRC waveform. Motivated by the above reasons, there are many proposed DFRC waveform designs on conventional OFDM systems [25]–[35]. Authors in [25] use spectral nulling technique to design DFRC waveform by minimizing peak side-lobes (PSL) in the time domain. Some other waveform designs optimize power allocation across subcarriers by jointly considering achievable capacity and various radar performance metrics [26]–[30]. Specifically [26] and [27] studies waveform design by optimizing mutual information (MI) for radar performance, authors in [28] propose a design regarding Cramér-Rao bound (CRB), and proposed design in [29] optimizes signal-to-noise power ratio (SNR) while [30] features false alarm probability as their optimization radar metric. In recent literature, joint subcarrier selection and power allocation strategies for DFRC waveform design are developed in [31]–[35]. Waveform designs that adopted subcarrier selection and power allocation approaches are classified on which radar metric they have considered. MI based approaches include [31]–[33] while the most recent works [34] and [35] proposed CRB minimized optimal waveforms.

In the subcarrier selection and power allocation approach,

The work of H. Arslan was supported by the Scientific and Technological Research Council of Turkey (TUBITAK) under Grant 120C142.

E. Memisoglu, T. Yılmaz, and H. Arslan are with the Department of Electrical and Electronics Engineering, Istanbul Medipol University, 34810 Istanbul, Turkey. E-mail: ebubekir.memisoglu@std.medipol.edu.tr, {talha.yilmaz, huseyinarslan}@medipol.edu.tr

optimum power allocation for selected radar and communication subcarriers is done through formulated optimization problems based on the adopted scenario. However, proposed joint subcarrier selection and power allocation based methods either exploits certain opportunities like low traffic load by using empty subcarriers as radar dedicated subcarriers in [34] or requires standards support due to novel frame structures and signalling approaches such as proposed in [35]. Moreover, CRB-based formulations generally yield non-convex problems [31] which leads into computationally expensive solutions.

Motivated by the drawbacks above, this paper proposes a novel OFDM DFRC waveform design inspired by active constellation extension [36]. The proposed power allocation via constellation extension does not affect receiver signal processing which we refer as transparency. The transparency property of the proposed method allows power allocation of communication data subcarriers without any feedforward signaling. Thus, the proposed method can improve theoretical communication and radar performance by allocating more power to any conventional OFDM frame structure by utilizing the constellation extension without extra signaling or affecting the receiver. The main contributions of this work are summarized as follows:

- A transparent waveform design to the communication receiver in DFRC systems is proposed, which can be implemented directly in the current wireless standards.
- An unique power allocation method for waveform design is proposed where only the power levels of the data symbols that has been modulated with the outer points of the constellation is enhanced, resulting with improved communication and radar performance.
- A novel method is developed to find the subcarrier indices for the power enhancement in the waveform design.
- Symbol error rate (SER) expressions are derived analytically for the designed waveform to analyze the impact of the proposed algorithm on the communication performance in the OFDM DFRC system. Also, the complexity analysis of the proposed method is performed.

The rest of the paper is organized as follows. Section II collectively describes the considered DFRC system and signal model. Section III provides the mathematical expressions of delay and Doppler CRBs and explains the proposed waveform design. Section IV derives the theoretical SER and computational complexity expressions for the performance analysis of the proposed waveform design. Section V provides simulation results for the evaluation of radar and communication performance. Finally, Section VI concludes this paper. [1]

[1] *Notation:* Bold, lowercase and capital letters denote the signal vectors and matrices, respectively. $\Re\{.\}$ is the real part of a complex signal. $(.)^T$ and $(.)^H$ denote transposition and Hermitian transposition, respectively. $\odot$ and $\otimes$ denote the Hadamard and tensor product, respectively. $\mathbf{1}_M$ is an one vector with the size M. $\mathcal{CN}(0,\sigma^2)$ denotes the circularly symmetric complex Gaussian distribution with 0 mean and variance σ^2. $\|.\|_\infty$ denotes the infinity norm of a vector. The floor function is denoted by $\lfloor . \rfloor$. The function vec(.) converts a matrix into vector form. The function $sort(.)$ sorts the elements of a vector in ascending order and returns the sorted vector. The function $mod(a,m)$ returns the remainder after division of a by m, where a is the dividend and m is the divisor. The complementary error function is denoted by $Q(x) = \int_x^\infty \frac{2}{\sqrt{\pi}} e^{-x^2} dx$.

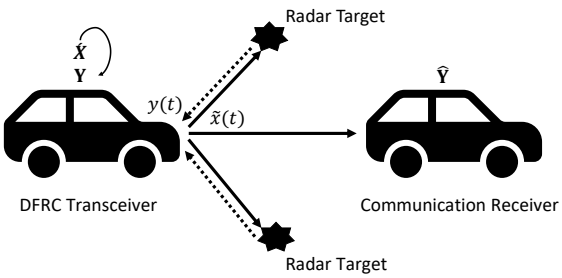

Fig. 1: The considered system model with DFRC transceiver, communication receiver, and radar targets.

II. System Model

A DFRC system for a vehicular wireless communication is considered as described in Fig. 1. The transceiver concurrently transmits OFDM symbols to a communication receiver with single antenna and senses the radar parameters of range and velocity using the reflected signals from radar targets in the environment. Since the transmitter and radar receiver operates on a single hardware, the properties of transmitted signal are perfectly known by radar receiver. Also, a DFRC transceiver with ideal transmitter-receiver isolation is assumed where the self interference due to full duplex radar process can be cancelled significantly by available techniques in the literature [37], [38].

A. Transmit Signal Model

A frame of OFDM waveform is generated to perform communication and radar-sensing concurrently. This frame consists of M OFDM symbols and N subcarriers per each symbol. Here, the symbol duration and subcarrier spacing is denoted by T and $\Delta f = 1/T$, respectively. On the n-th subcarrier of m-th symbol, the modulated complex data symbols of D-quadrature amplitude modulation (QAM) are represented by $X(n,m)$. Then, the m-th baseband OFDM signal with a cyclic prefix (CP) addition is given as

$$x_m(t) = \frac{1}{N} \sum_{n=0}^{N-1} X(n,m) e^{j2\pi n \Delta f t} \text{rect}\left(\frac{t - mT_s}{T_s}\right), \quad (1)$$

where $T_s = T + T_{cp}$ and T_{cp} denote the total OFDM symbol duration and CP duration, respectively. The rectangular function rect(t) takes the value 1 for $t \in [0, T_s]$ and 0 otherwise. Also, the T_{cp} duration is larger than the maximum excess delay of the communication and radar channel to maintain circular convolution and avoid inter-symbol interference. Transceiver uses the reflections of the communication signal to obtain unbiased estimates of radar parameters. Lower CRBs implies better parameter estimation performance. Thus, the proposed method increases the power level of the conventional OFDM subcarriers ($X(n,m)$) to decrease the delay and Doppler CRBs. We define $\acute{\mathbf{X}} \in \mathbb{C}^{N \times M}$ as the obtained subcarriers after power modification process with the elements $\acute{X}(n,m)$.

Performance metrics CRB and SER will be calculated over $\acute{\mathbf{X}}$ to evaluate performance of the proposed method. Using this notation, the baseband signal model for the proposed OFDM system is obtained as

$$\acute{x}_m(t) = \frac{1}{N}\sum_{n=0}^{N-1} \acute{X}(n,m) e^{j2\pi n \Delta f t} \text{rect}\left(\frac{t - mT_s}{T_s}\right). \quad (2)$$

Proposed method will change the powers of only some of the subcarriers due to the power budget constraint. Power of a modified subcarrier can be denoted as $|\acute{X}(n,m)|^2$. On the other hand, power of an unmodified subcarrier is $|X(n,m)|^2$ which is dependent on the used modulation. Then, the baseband signal is converted to the passband signal and transmitted via an antenna as

$$\tilde{x}(t) = \Re\left\{\sum_{m=0}^{M-1} \acute{x}_m(t) e^{j2\pi f_c t}\right\}, \quad (3)$$

where f_c is the carrier frequency of the transmitted signal.

B. Radar Receiver

Suppose there are K radar targets in the environment. The reflected signal from the k-th target is received with a delay τ_k and normalized Doppler shift $\nu_k \triangleq 2v_k/c$ where v_k and c are the radial velocity and the speed of propagation, respectively. The reflected signal has an attenuation factor h_k including path loss, reflection and processing gains. Then, after down-conversion operation, the downconverted signal at the radar receiver can be expressed as [39]

$$\begin{aligned} y(t) &= \sum_{k=0}^{K-1}\sum_{m=0}^{M-1} h_k \acute{x}_m(t-\tau_k) e^{j2\pi f_c \nu_k t} + w(t), \\ &\approx \sum_{k=0}^{K-1}\sum_{m=0}^{M-1} h_k \acute{x}_m(t-\tau_k) e^{j2\pi f_c \nu_k m T_s} + w(t), \end{aligned} \quad (4)$$

where $w(t)$ is the additive noise and the approximation in (4) is done by assuming $f_c \nu_k T_s \ll 1$ so that the phase rotation within one OFDM symbol is approximately constant. After the CP removal, the Fourier transform is applied to the m-th OFDM symbol and then the received signal in the frequency domain is obtained as [39]

$$\begin{aligned} Y(n,m) = \acute{X}(n,m) &\sum_{k=0}^{K-1} h_k e^{-j2\pi n \Delta f \tau_k} e^{j2\pi f_c \nu_k m T_s} \\ &+ Z(n,m), \end{aligned} \quad (5)$$

where $Z(n,m)$ is the additive white Gaussian noise (AWGN) sample with $\mathcal{CN}(0,\, \sigma_r^2)$. Denoting the frequency and time steering vectors as

$$\boldsymbol{\theta}(\tau) \triangleq [1, e^{-j2\pi\Delta f \tau}, \ldots, e^{-j2\pi(N-1)\Delta f \tau}]^T, \quad (6)$$

$$\boldsymbol{\phi}(\nu) \triangleq [1, e^{-j2\pi f_c T_s \nu}, \ldots, e^{-j2\pi f_c (M-1) T_s \nu}]^T. \quad (7)$$

Accordingly, plugging (6) and (7) into (5), the received signal in matrix form can be written as

$$\mathbf{Y} = \acute{\mathbf{X}} \odot \sum_{k=0}^{K-1} \alpha_k \boldsymbol{\theta}(\tau_k) \boldsymbol{\phi}^H(\nu_k) + \mathbf{Z}, \quad (8)$$

where $\mathbf{Y} \in \mathbb{C}^{N\times M}$ and $\mathbf{Z} \in \mathbb{C}^{N\times M}$ are the matrices of $Y(n,m)$ and $Z(n,m)$, respectively. Transceiver obtains the unbiased estimates of the unknown target parameters which are delays (τ_k) and Doppler shifts (ν_k), using the measurements $Y(n,m)$ given the transmitted symbols ($\acute{X}(n,m)$) are known at the transceiver. The CRB metric is used to evaluate estimation performance for these parameters at the transceiver.

C. Communication Receiver

After the down-conversion of the received signal to baseband, the CP removal and fast Fourier transform (FFT) operations are performed for each OFDM symbol at the communication receiver. Then, the received signal in the frequency domain similar to (8) can be written as

$$\widehat{\mathbf{Y}} = \acute{\mathbf{X}} \odot \widehat{\mathbf{H}} + \widehat{\mathbf{Z}}, \quad (9)$$

where $\widehat{\mathbf{H}} \in \mathbb{C}^{N\times M}$ represents Rayleigh channel frequency response factors of the communication channel with $\mathcal{CN}(0,\, 1)$ and $\widehat{\mathbf{Z}} \in \mathbb{C}^{N\times M}$ is the AWGN matrix with $\mathcal{CN}(0,\, \sigma_c^2)$. At communication receiver, a perfect channel state information is assumed for channel equalization. The equalized data symbols are decoded to obtain the transmitted data symbols. Although a perfect channel state information is considered at the communication receiver in the system model, an imperfect channel state information will have a same degradation for conventional OFDM and proposed method because the proposed method only modify the data symbols, not the pilot symbols. As a result, channel estimation performance will be identical for conventional OFDM and proposed method.

III. Waveform Design

In this section, the calculation of the delay and Doppler CRBs are provided and the proposed waveform design is explained in detail.

A. CRBs of Delay and Doppler Estimation

Proposed waveform design considers delay and Doppler CRBs to improve radar performance. The waveform design to increase the radar performance by minimizing the CRBs requires a proper power allocation. The power level of data symbols in the frame are represented by the matrix $\mathbf{P} \in \mathbb{C}^{N\times M}$, and the vector form of $\mathbf{P}$ is denoted as $\mathbf{q} \triangleq \text{vec}\,(\mathbf{P})$. Then, the CRBs of unbiased estimates $\widehat{\tau}$ and $\widehat{\nu}$ for delay and Doppler estimation in single target case can be calculated as [35]

$$\text{var}\,(\widehat{\tau}) \geq \text{C}_\tau = \frac{1}{2\gamma_r} \frac{(\mathbf{1}^T\mathbf{q})(\mathbf{q}^T\boldsymbol{\Upsilon}_\nu\mathbf{q})}{(\mathbf{q}^T\boldsymbol{\Upsilon}_\tau\mathbf{q})(\mathbf{q}^T\boldsymbol{\Upsilon}_\nu\mathbf{q}) - (\mathbf{q}^T\boldsymbol{\Upsilon}_{\tau\nu}\mathbf{q})^2}, \quad (10)$$

$$\text{var}\,(\widehat{\nu}) \geq \text{C}_\nu = \frac{1}{2\gamma_r} \frac{(\mathbf{1}^T\mathbf{q})(\mathbf{q}^T\boldsymbol{\Upsilon}_\tau\mathbf{q})}{(\mathbf{q}^T\boldsymbol{\Upsilon}_\tau\mathbf{q})(\mathbf{q}^T\boldsymbol{\Upsilon}_\nu\mathbf{q}) - (\mathbf{q}^T\boldsymbol{\Upsilon}_{\tau\nu}\mathbf{q})^2}, \quad (11)$$

This article has been accepted for publication in IEEE Transactions on Vehicular Technology. This is the author's version which has not been fully edited and content may change prior to final publication. Citation information: DOI 10.1109/TVT.2023.3281130

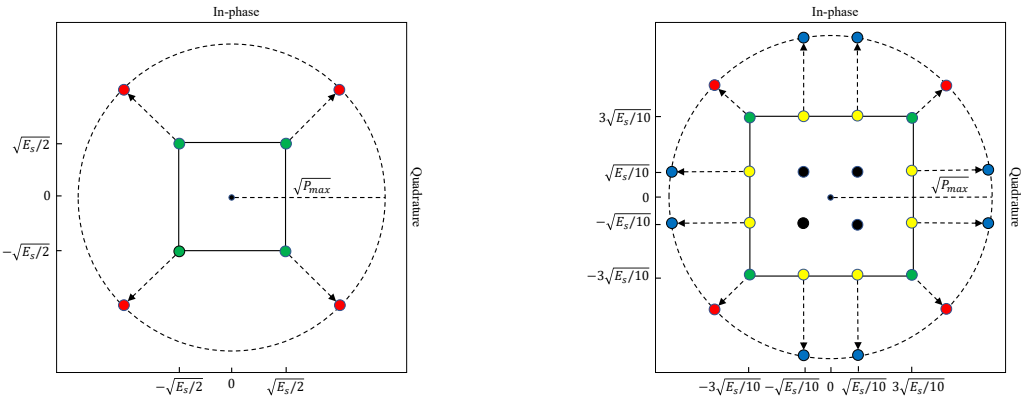

Fig. 2: The scatter plots of the proposed waveform design for QPSK and 16-QAM constellation. The black, yellow and green circles belong to conventional constellation, and blue and red circles are due to the proposed method.

where

$$\begin{aligned}
\mathbf{u}_\tau &\triangleq 2\pi\Delta f(\mathbf{1}_M \otimes \xi_N),\\
\mathbf{u}_\nu &\triangleq 2\pi f_c T_s(\xi_M \otimes \mathbf{1}_N),\\
\boldsymbol{\Upsilon}_\tau &\triangleq (\mathbf{u}_\tau \odot \mathbf{u}_\tau)\,\mathbf{1}_{NM}^T - \mathbf{u}_\tau\mathbf{u}_\tau^T,\\
\boldsymbol{\Upsilon}_\nu &\triangleq (\mathbf{u}_\nu \odot \mathbf{u}_\nu)\,\mathbf{1}_{NM}^T - \mathbf{u}_\nu\mathbf{u}_\nu^T,\\
\boldsymbol{\Upsilon}_{\tau\nu} &\triangleq (\mathbf{u}_\tau \odot \mathbf{u}_\nu)\,\mathbf{1}_{NM}^T - \mathbf{u}_\tau\mathbf{u}_\nu^T.
\end{aligned}$$

Here, γ_r is the SNR at the radar receiver and $\xi_N = [0, 1, \ldots, N-1]$. As seen from (10) and (11), the CRBs depend on $\mathbf{q}$, γ_r, Δf, f_c, and T_s. Since the parameters of γ_r, Δf, f_c, and T_s are system parameters for a target delay and Doppler estimation, only $\mathbf{q}$ is changed for the CRBs minimization in the waveform design.

B. Proposed Waveform Design

The minimization of the joint delay and Doppler CRBs involves optimization of the OFDM subcarrier powers. In conventional OFDM systems, the $\mathbf{P}$ matrix is formed by the power of the modulated data symbols based on the D-QAM, and they have a total power of P_c. On the other hand, since the power of data symbols are increased to improve the radar performance by minimizing the CRBs, the data symbols in the frame will have a total power of P_t where $P_t > P_c$. In the proposed waveform design, only OFDM data symbols are used for the power optimization. Therefore, separate subcarriers as in [34] are not assigned for the radar performance improvement. Also, a power threshold P_{max} for data symbols is considered in the CRB minimization for the following reasons: Firstly, the transmit signal requires to be a spectrum mask compliant. Accordingly, if there is a large power difference between subcarriers, the average signal power needs to be decreased so that the subcarriers with highest power level are compliant with spectrum mask. However, this will not be a power efficient. Secondly, if there is an inter-carrier interference in the system, the interference of high power subcarriers affects other subcarriers significantly for the communication performance. Lastly, if the ratio of the maximum power to the average power increases, the side-lobe level of ambiguity function also increases [40].

Owing to the fact that there are the constraints of P_t and P_{max} in the system for optimum CRB minimization, the subcarrier indices to obtain the optimum CRBs need to be found for the power allocation. These subcarrier indices are represented with the set R_m for the m-th OFDM symbol and the subcarriers in R_m have power allocation of P_{max}. Therefore, the power allocation problem for the optimum CRB minimization can be formulated as

$$\min_{\mathbf{q}} \quad \lambda C_\tau + (1-\lambda)C_\nu \tag{12a}$$

$$\text{s.t.} \quad \mathbf{1}_{NM}^T\mathbf{q} = P_t, \quad \mathbf{q} \succeq 0, \tag{12b}$$

$$P(n,m) = P_{max},\ n \in R_m,\ \forall m, \tag{12c}$$

where λ denotes the determined weighting factor for delay Doppler estimation accuracy. For instance, if $\lambda = 1$, the optimization only minimizes the CRB for the delay estimation. Note that there is a relationship between $\mathbf{q}$ and $\mathbf{P}$ as $\mathbf{q} \triangleq \text{vec}\,(\mathbf{P})$. As deduced from (12a), the R_m set requires to be found and then the power allocation to the subcarrier indices in R_m is performed to obtain $\mathbf{q}$. In order to modify every subcarrier power to the same power level, we introduce the constraint (12c). The constraint (12c) forces the algorithm to allocate the same amount of power for each selected subcarrier. Allocating power in this manner also forces power distribution to be more uniform, which decreases integrated side-lobe level and improves radar accuracy.

The power allocation to data symbols of D-QAM on the selected subcarriers for the proposed method is illustrated for the quadrature phase shift keying (QPSK) and 16-QAM constellation in Fig. 2. The symbol alphabet of D-QAM is defined as $\mathcal{S} = \{\pm(2d+1) \pm (2d+1)j\}$ with $d = \{0, 1, \ldots, \sqrt{D}/2-1\}$. For the power allocation in the proposed method, $\mathcal{S}$ is divided into three subsets as $\mathcal{S}_1$, $\mathcal{S}_2$ and $\mathcal{S}_3$. The subsets $\mathcal{S}_1$, $\mathcal{S}_2$ and $\mathcal{S}_3$ have the data points of the D-QAM constellation in the inside (black colored circles), in the corner (green colored circles), and neither in the inside nor in the corner (yellow colored circles), respectively. As seen from the figure, the power levels of data points in $\mathcal{S}_2$ and $\mathcal{S}_3$ are increased in the proposed method. Therefore, the sets of empowered data symbols of $\mathcal{S}_2$ and $\mathcal{S}_3$ are denoted by $\mathcal{C}_1$

(red colored circles) and $\mathcal{C}_2$ (blue colored circles), respectively. Also, the data symbols of $\mathcal{S}_2$ and $\mathcal{S}_3$ are highlighted by a inside rectangle as seen in Fig. 2. The data symbols of D-QAM constellation have the average power of E_s and the normalization factor is calculated as $\sqrt{(2\,(D-1)\,/3)}$.

To design the $\mathbf{q}$ vector for the optimum CRB minimization, firstly, the total number of subcarriers for the power allocation is required to be determined. The number depends on the parameters of P_c, P_t, P_{max} and D-QAM. In the proposed method, the power levels of only data symbols in $\mathcal{S}_2$ and $\mathcal{S}_3$ are increased. The power levels of the d_2-th and d_3-th data symbol in $\mathcal{S}_2$ and $\mathcal{S}_3$ are represented by P_{d_2} and P_{d_3} where $d_2 = \{0, 1, \ldots, D_2 - 1\}$ and $d_3 = \{0, 1, \ldots, D_3 - 1\}$, respectively. Therefore, the total number of subcarriers with a P_{max} power level can be calculated as

$$N_R = \left\lfloor \frac{(P_t - P_c)\,(D_2 + D_3)}{\sum_{d_2=0}^{D_2-1}(P_{max} - P_{d_2}) + \sum_{d_3=0}^{D_3-1}(P_{max} - P_{d_3})} \right\rfloor. \tag{13}$$

The probability of a data symbol in $\mathcal{S}_2 \cup \mathcal{S}_3$ is calculated as $\frac{1}{(D_2+D_3)}$. For instance, QPSK constellation has the parameters of $D_2 = 4$ and $D_3 = 0$, and the probability of $\frac{1}{4}$, on the other hand, the 16-QAM constellation has the parameters of $D_2 = 4$ and $D_3 = 8$, and the probability of $\frac{1}{12}$ as seen from Fig. 2. In the case of constant P_t, P_c and D, if P_{max} increases, N_R decreases.

After calculating the N_R, the N_R subcarrier indices among MN subcarrier indices are required to be selected for an optimum CRB optimization. Then, the proposed method allocates a power level of P_{max} to the selected subcarriers. Note that P_{max} is always larger than the power of the data symbols on the selected subcarrier. To find the optimum $\mathbf{q}$ in Eq. (12a), the number of different combinations for brute-force search is calculated as $\frac{(MN)!}{N_R!(MN-N_R)!}$. Therefore, the brute-force search is not feasible in a practical system. For instance, the approximate number of 4.48×10^{306} searches are required to find the optimum $\mathbf{q}$ vector with brute-force search for the parameters of $N = 64$, $M = 16$, and $N_R = 512$. As inferred from Eqs. (10) and (11), all subcarriers are independent of each other and the power enhancement of each subcarrier contributes to the CRB minimization positively. It means that the power enhancement of any subcarrier minimizes the CRBs of delay and Doppler estimation. However, the power enhancement of each subcarrier contributes differently on the CRB minimization. This feature is also mentioned in [34] and [35]. For instance, the edge-most subcarriers are optimum for the delay CRB minimization, on the other hand, the edge-most OFDM symbols are optimum for the Doppler CRB minimization [34]. Also, as deduced from the proof of joint delay and Doppler optimization algorithm in [34], it is concluded that the subcarriers in the frame contribute independently to CRB minimization. Therefore, finding the CRB minimization performance of each subcarrier provides the optimum solution for the selection of the N_R subcarrier indices.

The matrix $\mathbf{G} \in \mathbb{R}^{N \times M}$ of the weight factors is obtained based on the CRB minimization of each subcarrier as described in Algorithm 1. Firstly, the system parameters of f_c, Δf, T_s, γ_r, N, M, P_{max} and λ are determined. If the system parameters are constant for a different frame generation, same $\mathbf{G}$ matrix can be used to select the subcarrier indices for CRB minimization. For a fair evaluation, a unit power level is assigned to all subcarriers in the beginning as $\bar{\mathbf{P}} = \mathbf{1}_{N \times M}$. Then, the power level of the n-th subcarrier of the m-th OFDM symbol is increased to P_{max} as $\bar{P}(n, m) = P_{max}$. Next, the $\bar{\mathbf{P}}$ matrix is vectorized to $\bar{\mathbf{q}} \triangleq \text{vec}\left(\bar{\mathbf{P}}\right)$. Afterwards, according to the minimization problem in (12a), the weight factor for the n-th subcarrier of the m-th OFDM symbol is found as $G_{n,m} = \lambda C_\tau + (1 - \lambda) C_\nu$. Note that only one element with P_{max} is available in $\bar{\mathbf{q}}$, and other elements have unit power level for each iteration. After finding the weight factors for each subcarrier indices in the frame, the matrix $\mathbf{G}$ is formed. Since the matrix $\mathbf{G}$ indicates the performance of CRB minimization for the subcarrier indices, the indices with lower values in $\mathbf{G}$ are more efficient for the minimization problem in (12a). Although the subcarrier selection algorithms in [34] can be also used for the proposed waveform design instead of Algorithm 1, the advantage of the algorithm is to provide an optimum subcarrier selection for any λ values unlike in [34].

The CRB improvement for better radar performance is achieved by increasing the power level of subcarriers in $\mathbf{X}$ for the proposed method. The proposed method exploits the modulation constellation to increase the power level of data symbols, and provides a transparent operation to the

Algorithm 1 The matrix generation of weight factors.

```
Define f_c, Δf, T_sym, γ_r, N, M, P_max and λ
Set n = 0
while n ≤ N − 1 do
    Set m = 0
    while m ≤ M − 1 do
        P̄ = 1_{N×M}
        P̄(n, m) = P_max
        q̄ ≜ vec(P̄)
        G(n, m) = λC_τ + (1 − λ)C_ν
        m ← m + 1
    end while
    n ← n + 1
end while
```

Algorithm 2 Proposed waveform design.

```
Define P_t, P_c, N, M, P_max and D
Set i = 0 and X́ = X
Calculate N_R in (13)
Find the G matrix by Algorithm 1
while i ≤ N_R − 1 do
    g ≜ vec(G)
    [ǵ, I] = sort(g)
    n = mod(I(i), N)
    m = ⌊(I(i))/M⌋
    if X(n, m) ∈ S_2 then
        X́(n, m) = √P_max X(n,m)/|X(n,m)|
    elseif X(n, m) ∈ S_3 then
        X́(n, m) = X(n, m) + A_{d_3}
    else
        X́(n, m) = X(n, m)
    end if
    i ← i + 1
end while
```

communication receiver as in [36]. Therefore, same processes at the receiver with conventional OFDM systems are required for the proposed method. To achieve this, the proposed method only increases the power levels of data symbols in $\mathcal{S}_2 \cup \mathcal{S}_3$ as shown in Fig. 2. In the figure, the constellations of QPSK and 16-QAM are described. For the QPSK modulation, all data symbols are on the outer of the constellation so that all subcarriers in $\mathbf{X}$ are suitable for the power enhancement. Hence, if the data symbols on the constellation diagram have same power level and different phases as in phase shift keying modulation, the proposed method can use all data symbols for the power enhancement. On the other hand, if the data symbols on the constellation diagram have different power levels and phases as in 16-QAM, only the outer data symbols in $\mathcal{S}_2 \cup \mathcal{S}_3$ can be used to minimize the CRB.

The proposed waveform design is performed as described in Algorithm 2. In the algorithm, firstly, the system parameters of P_t, P_c, N, M, P_{max} and D are determined. After calculating N_R in (13) and finding the $\mathbf{G}$ matrix in Algorithm 1, the power enhancement of N_R subcarriers starts. To find the $\mathbf{q}$ in the proposed method, the subcarrier indices according to $\mathbf{G}$ should be sorted. For the sorting, the vector form of $\mathbf{G}$ as $\mathbf{g} \triangleq \text{vec}\,(\mathbf{G})$ is used. The corresponding indices of $\mathbf{g}$ as $\bar{\mathbf{g}} \in \mathbb{R}^{NM\times 1}$ and $\mathbf{I} \in \mathbb{N}^{NM\times 1}$, respectively. The indices of the i-th subcarrier for the power enhancement in the terms of n and m are calculated as $n = mod(I(i), N)$ and $m = \lfloor I(i)/M \rfloor$, where $i = \{0, 1, \ldots, NM-1\}$. Afterwards, check the data symbol on $X(n,m)$, if it is in $\mathcal{S}_2$, then change its power level to P_{max} as $\acute{X}(n,m) = \sqrt{P_{max}}\frac{X(n,m)}{|X(n,m)|}$. If it is in $\mathcal{S}_3$, add a complex value A_{d_3} to $X(n,m)$ for the d_3-th data symbol in $\mathcal{S}_3$ so that $\acute{X}(n,m) = X(n,m) + A_{d_3}$ have the power level of P_{max}. If it is in $\mathcal{S}_1$, do not change the power level as $\acute{X}(n,m) = X(n,m)$. After the power levels of data symbols on the N_R subcarriers are increased, the matrix $\acute{\mathbf{X}}$ is obtained. Note that the modifications on $\mathbf{X}$ to obtain $\acute{\mathbf{X}}$ optimize $\mathbf{q}$ in Eq. (12a) and are transparent to the communication receiver. Therefore, if the system requires to enhance radar performance by minimizing the CRBs of delay and Doppler estimations, the proposed method can meet this requirement without a channel state information at the DFRC transceiver and a feedforward signaling to the communication receiver.

IV. Performance Analysis

In this section, the theoretical SER and computational complexity analysis are investigated. Firstly, the average SER of conventional OFDM is provided, and then the average SER of the proposed method is obtained. Secondly, the computational complexity of the proposed waveform design is calculated.

A. SER Analysis

The received signal on the n-th subcarrier of m-th conventional OFDM symbol at the communication receiver is given as

$$\widehat{Y}(n,m) = X(n,m)\widehat{H}(n,m) + \widehat{Z}(n,m), \tag{14}$$

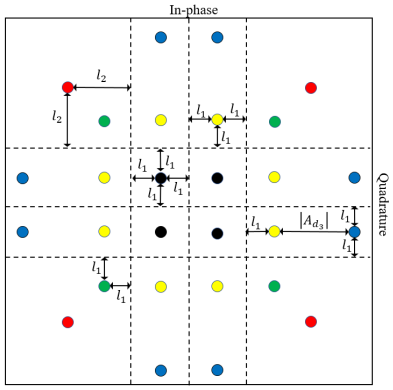

Fig. 3: The minimum distances to the decision boundaries (dashed lines) in the constellation of the proposed method for D-QAM.

where the probability distribution function of the Gaussian random variable $z = \Re\{\widehat{Z}(n,m)\}$ with the 0 mean and variance $\sigma_c^2/2$ is

$$p(z) = \frac{1}{\sqrt{\pi\sigma_c^2}} e^{-\frac{z^2}{\sigma_c^2}}. \tag{15}$$

Then, the instantaneous SNR can be written as

$$\gamma_c(n,m) = \frac{|X(n,m)|^2|\widehat{H}(n,m)|^2}{\sigma_c^2}. \tag{16}$$

Afterwards, the average SNR per data symbol is found by taking the expected value of (16) as $\bar{\gamma}_c = \frac{E_s}{\sigma_c^2}$. After the $\bar{\gamma}_c$ is obtained, the closed-form expression of average SER for D-QAM over Rayleigh fading channels is given as [41]

$$P_s(E) = 2\left(\frac{\sqrt{D}-1}{\sqrt{D}}\right)(1-\beta) - \left(\frac{\sqrt{D}-1}{\sqrt{D}}\right)^2\left[1-\beta\left(\frac{4}{\pi}tan^{-1}\left(\frac{1}{\beta}\right)\right)\right], \tag{17}$$

where $\beta = \sqrt{\frac{1.5\bar{\gamma}_c}{D-1+1.5\bar{\gamma}_c}}$.

In the constellation of the proposed method, the data symbols belong to the sets of $\mathcal{S}_1$, $\mathcal{S}_2$, $\mathcal{S}_3$, $\mathcal{C}_1$ and $\mathcal{C}_2$. As seen from Fig. 3, the data symbols in these sets have different the minimum distances to the decision boundaries and the number of decision boundaries. Therefore, the minimum distances to decision boundaries for the data symbols in $\mathcal{S}_1$, $\mathcal{S}_2$, $\mathcal{S}_3$, $\mathcal{C}_1$ and $\mathcal{C}_2$ are (l_1, l_1, l_1, l_1), (l_1, l_1), (l_1, l_1, l_1), (l_2, l_2), and $(l_1, l_1, |A_{d_3}| + l_1)$ as shown in the figure. The distances of l_1 and l_2 are calculated as $l_1 = \sqrt{3E_s/(2(D-1))}$ and $l_2 = \sqrt{P_{max}/2} - (\sqrt{D}-2)l_1$. Although each data symbol in $\mathcal{S}_1$, $\mathcal{S}_2$, $\mathcal{S}_3$, and $\mathcal{C}_1$ have same minimum distances to decision boundaries, the data symbols in $\mathcal{C}_2$ may have different minimum distances. However, each data symbol in $\mathcal{C}_2$ have same minimum distances for 16-QAM, and $|A_{d_3}|$ is calculated as $|A_{d_3}| = \sqrt{(P_{max} - l_1^2)} - 3l_1$ for all d_3 indices.

To calculate the average SER of the proposed method, firstly, the individual SER of each data symbol on the constellation of D-QAM is calculated, and then the average SER

is found from the individual SERs. These data symbols belong to the sets of $\mathcal{S}_1$, $\mathcal{S}_2$, $\mathcal{S}_3$, $\mathcal{C}_1$, and $\mathcal{C}_2$. The data symbols on each set except in $\mathcal{C}_2$ have same SER performance. The SERs of D-QAM data symbols according to their sets for a channel factor $h = \widehat{H}(n,m)$ are given as [42] [43]

$$\dot{P}_s(E|\mathcal{S}_1) = 1 - \left(1 - \frac{1}{2}Q\left(\sqrt{\frac{l_1^2|h|^2}{\sigma_c^2}}\right) - \frac{1}{2}Q\left(\sqrt{\frac{l_1^2|h|^2}{\sigma_c^2}}\right)\right) \times \left(1 - \frac{1}{2}Q\left(\sqrt{\frac{l_1^2|h|^2}{\sigma_c^2}}\right) - \frac{1}{2}Q\left(\sqrt{\frac{l_1^2|h|^2}{\sigma_c^2}}\right)\right), \tag{18}$$

$$\dot{P}_s(E|\mathcal{S}_2) = 1 - \left(1 - \frac{1}{2}Q\left(\sqrt{\frac{l_1^2|h|^2}{\sigma_c^2}}\right)\right) \times \left(1 - \frac{1}{2}Q\left(\sqrt{\frac{l_1^2|h|^2}{\sigma_c^2}}\right)\right), \tag{19}$$

$$\dot{P}_s(E|\mathcal{S}_3) = 1 - \left(1 - \frac{1}{2}Q\left(\sqrt{\frac{l_1^2|h|^2}{\sigma_c^2}}\right) - \frac{1}{2}Q\left(\sqrt{\frac{l_1^2|h|^2}{\sigma_c^2}}\right)\right) \times \left(1 - \frac{1}{2}Q\left(\sqrt{\frac{l_1^2|h|^2}{\sigma_c^2}}\right)\right), \tag{20}$$

$$\dot{P}_s(E|\mathcal{C}_1) = 1 - \left(1 - \frac{1}{2}Q\left(\sqrt{\frac{l_2^2|h|^2}{\sigma_c^2}}\right)\right) \times \left(1 - \frac{1}{2}Q\left(\sqrt{\frac{l_2^2|h|^2}{\sigma_c^2}}\right)\right), \tag{21}$$

$$\dot{P}_s(E|\mathcal{C}_2) = 1 - \left(1 - \frac{1}{2}Q\left(\sqrt{\frac{l_1^2|h|^2}{\sigma_c^2}}\right) - \frac{1}{2}Q\left(\sqrt{\frac{l_1^2|h|^2}{\sigma_c^2}}\right)\right) \times \left(1 - \frac{1}{2D_3}\sum_{d_3=0}^{D_3-1} Q\left(\sqrt{\frac{(|A_{d_3}| + l_1)^2|h|^2}{\sigma_c^2}}\right)\right). \tag{22}$$

Since the Rayleigh fading channel model is considered, the random variable $\varphi = |h|^2$ will has a probability distribution function of chi-square with two degrees of freedom as [43]

$$p(\varphi) = e^{-\varphi}, \quad \varphi \geq 0. \tag{23}$$

Then, the average SER of the data symbols on $\mathcal{S}_1$, $\mathcal{S}_2$, $\mathcal{S}_3$, $\mathcal{C}_1$, and $\mathcal{C}_2$ for a Rayleigh channel are calculated respectively as

$$\widehat{P}_s(E|\mathcal{S}_1) = \int_0^\infty \dot{P}_s(E|\mathcal{S}_1)p(\varphi)d\varphi, \tag{24}$$

$$\widehat{P}_s(E|\mathcal{S}_2) = \int_0^\infty \dot{P}_s(E|\mathcal{S}_2)p(\varphi)d\varphi, \tag{25}$$

$$\widehat{P}_s(E|\mathcal{S}_3) = \int_0^\infty \dot{P}_s(E|\mathcal{S}_3)p(\varphi)d\varphi, \tag{26}$$

$$\widehat{P}_s(E|\mathcal{C}_1) = \int_0^\infty \dot{P}_s(E|\mathcal{C}_1)p(\varphi)d\varphi, \tag{27}$$

$$\widehat{P}_s(E|\mathcal{C}_2) = \int_0^\infty \dot{P}_s(E|\mathcal{C}_2)p(\varphi)d\varphi. \tag{28}$$

To find the overall probability, the average probability of each set in the frame requires. Therefore, the occurrence probabilities of the sets in the frame are calculated as

$$P(\mathcal{S}_1) = \frac{\left(\sqrt{D}-2\right)\left(\sqrt{D}-2\right)}{D}, \tag{29}$$

$$P(\mathcal{S}_2) = \left(1 - P(\mathcal{S}_1) - \frac{N_R}{NM}\right)\left(\frac{1}{1+\sqrt{D}-2}\right), \tag{30}$$

$$P(\mathcal{S}_3) = \left(1 - P(\mathcal{S}_1) - \frac{N_R}{NM}\right)\left(\frac{\sqrt{D}-2}{1+\sqrt{D}-2}\right), \tag{31}$$

$$P(\mathcal{C}_1) = \left(\frac{N_R}{NM}\right)\left(\frac{1}{1+\sqrt{D}-2}\right), \tag{32}$$

$$P(\mathcal{C}_2) = \left(\frac{N_R}{NM}\right)\left(\frac{\sqrt{D}-2}{1+\sqrt{D}-2}\right). \tag{33}$$

Then, the overall average SER is calculated as

$$\begin{aligned}\widehat{P}_s(E) =& P(\mathcal{S}_1)\widehat{P}_s(E|\mathcal{S}_1) + P(\mathcal{S}_2)\widehat{P}_s(E|\mathcal{S}_2) \\ &+ P(\mathcal{S}_3)\widehat{P}_s(E|\mathcal{S}_3) + P(\mathcal{C}_1)\widehat{P}_s(E|\mathcal{C}_1) \\ &+ P(\mathcal{C}_2)\widehat{P}_s(E|\mathcal{C}_2).\end{aligned} \tag{34}$$

B. Complexity Analysis

The computational complexity of the proposed waveform design is calculated in the terms of real addition and multiplication operations based on Algorithm 1 and 2. Since the complexity of addition and subtraction, and the complexity of multiplication and division are similar, the operations of subtraction and division are considered addition and multiplication operations, respectively.

As seen from Algorithm 1, the addition and multiplication operations are only needed to obtain $G(n,m)$. Moreover, the calculations of C_τ and C_ν are required for $G(n,m)$, and C_τ and C_ν have same computational complexity. For the complexity of CRBs, the terms of $\mathbf{1}^T\mathbf{q}$ and $\mathbf{q}^T\boldsymbol{\Upsilon}_\tau\mathbf{q}$ are considered. Note that the complexity of $\mathbf{q}^T\boldsymbol{\Upsilon}_\tau\mathbf{q}$ is equivalent to $\mathbf{q}^T\boldsymbol{\Upsilon}_\nu\mathbf{q}$ and $\mathbf{q}^T\boldsymbol{\Upsilon}_{\tau\nu}\mathbf{q}$. The terms of $\mathbf{1}^T\mathbf{q}$ and $\mathbf{q}^T\boldsymbol{\Upsilon}_\tau\mathbf{q}$ have $(MN-1)$ additions, and $\left((MN)^2-1\right)$ additions and $\left((MN)^2+MN\right)$ multiplications, respectively. Therefore, the joint complexity of C_τ and C_ν is $2\left(5\left((MN)^2-1\right)+MN-1+1\right)$ additions and $2\left(5\left((MN)^2+MN\right)+6\right)$ multiplications. Since MN iterations, 1 addition, and 2 multiplications are required after the calculation of C_τ and C_ν, the total complexity of $G(n,m)$ is calculated as $10(MN)^3+2(MN)^2-9(MN)$ additions and $10(MN)^3+10(MN)^2+14(MN)$ multiplications. Note that Algorithm 1 is only required once for the transmission, and the $\mathbf{G}$ matrix obtained by Algorithm 1 can be used for next transmission if the system parameters are not changed.

In Algorithm 2, firstly, m and n are obtained with 2 multiplications in total. For one iteration, if $X(n,m)$ is the element of $\mathcal{S}_2$ or $\mathcal{S}_3$, the proposed power enhancement requires 2 multiplications or 1 addition, respectively. Otherwise, any operation is not required for $X(n,m)$. Since the probabilities of power-enhanced data symbols for $\mathcal{C}_1$ and $\mathcal{C}_1$ on D-QAM constellation are denoted by $P(\mathcal{C}_1)$ and $P(\mathcal{C}_2)$, the overall average complexity of Algorithm 2 can be calculated as $P(\mathcal{C}_2)N_R$ additions and $(2P(\mathcal{C}_1)N_R + 2N_R)$ multiplications.

This article has been accepted for publication in IEEE Transactions on Vehicular Technology. This is the author's version which has not been fully edited and content may change prior to final publication. Citation information: DOI 10.1109/TVT.2023.3281130

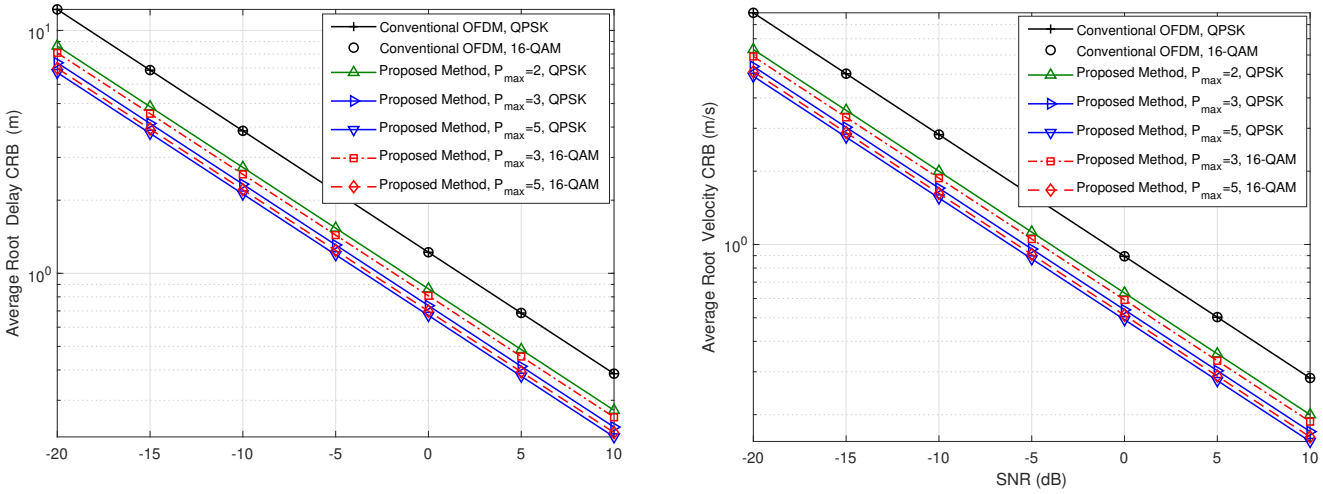

Fig. 4: The separate CRB optimization of the proposed waveform design for delay and Doppler estimation.

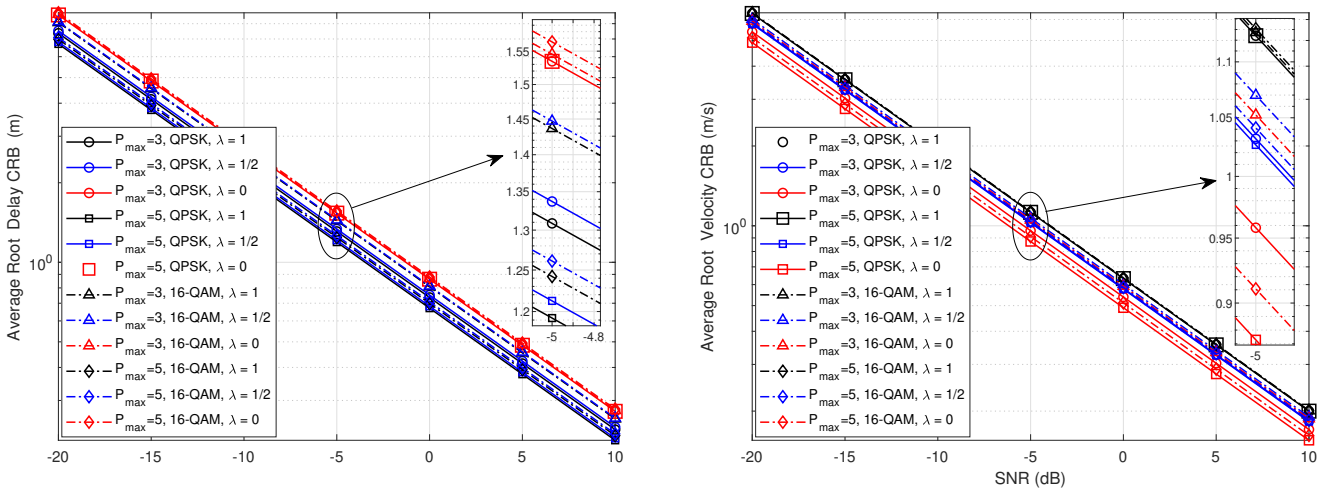

Fig. 5: The joint CRB optimization of the proposed waveform design for delay and Doppler estimation.

TABLE I: The parameter values for the OFDM signal.

Parameters	**Values**
Carrier frequency (f_c)	$2\ GHz$
Number of subcarriers (N)	64
Subcarrier spacing (Δf)	$23.4\ kHz$
Total symbol duration (T_s)	64 μs
Number of symbols (M)	16
Number of frames	10^5
Average signal power (E_s)	1
Total signal power (P_c)	NM
Total transmit signal power (P_t)	$2NM$

V. Simulation Results

In this section, the simulation results of the proposed waveform design are provided. The parameter values for the simulations are given in Table I. To observe the effects of different modulation orders in the proposed waveform design, QPSK ($D = 4$) and 16-QAM ($D = 16$) are used for the data symbols. The parameters E_s, P_c, and P_t are assigned based on the values of the QAM symbols in the frame. According to P_c and P_t, the different P_{max} values of 2, 3, and 5 are used for the CRB optimization. The radar SNR value is calculated as $\gamma_r = P_t/\sigma_r^2$. For the communication channel, a frequency selective channel with 4 taps is generated.

The performances of CRB optimization of delay and Doppler estimates with $\lambda = 1$ and $\lambda = 0$ are obtained in Fig. 4. Note that the waveform design optimization with $\lambda = 1$ considers the only delay CRB, and if $\lambda = 0$, then only Doppler CRB is considered for the optimization. The $P_{max} = 2$ value is used only for QPSK modulation, and all subcarriers have the P_{max} power level in that case. In the 16-QAM, $P_{max} = 2$ is not a feasible power level because the number of suitable subcarriers for the power enhancement in the proposed method is not sufficient to reach to P_t. The reason

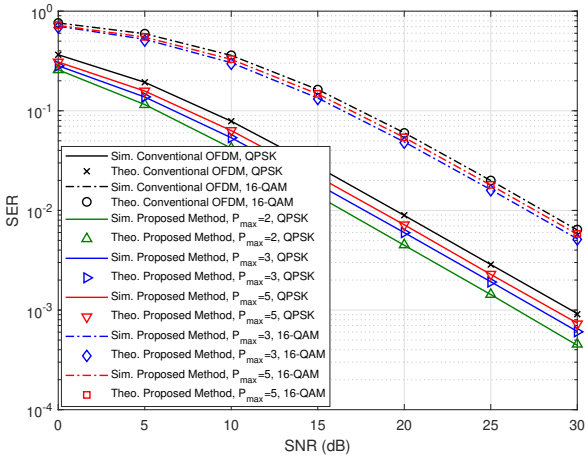

Fig. 6: SER performance of the proposed method for the comparison.

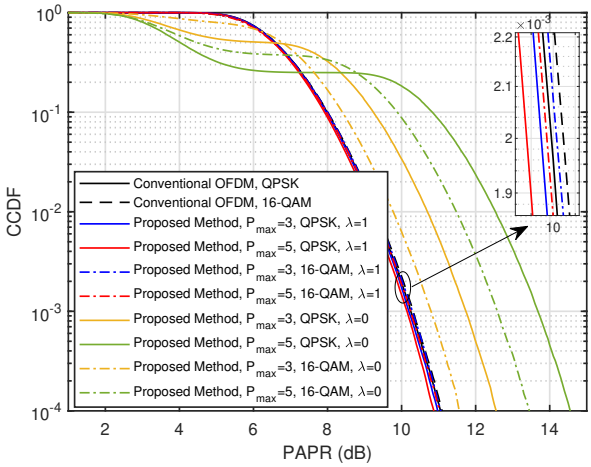

Fig. 7: PAPR performance of the proposed method for the comparison.

of using $P_{max} = 2$ is to show the effects of uniform power enhancement in the proposed method. As seen from the figure, if the P_{max} value increases, the CRB metric decreases for both delay and Doppler estimates. Therefore, a larger P_{max} value is better for the CRB minimization, but it should be limited in practical system due the reasons explained in Section III. The performance gains for delay and Doppler CRBs have similar characteristics. For the QPSK modulation, all OFDM data symbols have the same power level, and all of them are suitable for the power enhancement. On the other hand, for the 16-QAM modulation, the data symbols have different power levels although they have the same average power with QPSK. Therefore, the only data symbols on $\mathcal{S}_2$ and $\mathcal{S}_3$ are suitable for the power enhancement. Since some subcarriers indices with unsuitable data symbols are skipped for the power enhancement, the CRB minimization performance with 16-QAM is worse than the QPSK modulation. However, the gain difference decreases for larger P_{max} values.

The effects of λ on the CRBs of the proposed method with different modulation orders and P_{max} values are investigated in Fig. 5. If $0 < \lambda < 1$, the joint CRB optimization for delay and Doppler estimation is performed. If $\lambda = 1$, the best delay CRB performance is obtained, on the other hand, if $\lambda = 0$, the best Doppler CRB performance is obtained. The changing λ between 0 and 1 such as $\lambda = 1/2$ compromises between delay and Doppler CRB performances. Therefore, the decrease of λ increases the delay CRB while the Doppler CRB decreases. The change of CRB performance for a different λ value is not same for delay and Doppler estimates, and it depends on the system parameters such as f_c, N, M, and Δf. As seen from the figure, the change in λ affects the CRBs performance more if P_{max} is larger. Moreover, the change in λ affects the CRBs performance more if D is smaller.

The average SER performance of the proposed method compared to conventional OFDM are shown in Fig. 6. For symbol detection at the communication receiver, the same processes with conventional OFDM are deployed for the proposed method. As seen from the figure, the power enhancement of the subcarriers for CRB optimization also enhances the average SER performance because the proposed method increases the minimum distance between the data symbols on the constellation of D-QAM. For the case of $P_{max} = 2$ and QPSK, there is a uniform power enhancement and the best average SER performance is obtained for this case. As result, the average SER performance in the proposed method decreases when P_{max} increases as seen in Fig. 6. Although a larger P_{max} decreases the average SER for data symbols on $\mathcal{C}_1$ and $\mathcal{C}_2$, their occurrence probabilities on Eqs. (32) and (33) also decrease since number of enhanced subcarriers N_r decreases based on P_{max}. Moreover, when D increases the average SER performance gain of the proposed method compared to conventional OFDM decreases. Lastly, the simulation results of the proposed method and conventional OFDM are verified with the analytical results in (17) and (34) as seen from the figure.

The complementary cumulative distribution function (CCDF) performances of PAPR results for the proposed method with $\lambda = 1$ and $\lambda = 0$ are provided in Fig. 7. For $\lambda = 1$, the proposed method increases the power levels of the edge-most subcarriers of each OFDM symbol so that these OFDM symbols have the same average power. Although the proposed method with $\lambda = 1$ increases the power, a similar PAPR performance compared to conventional OFDM is obtained for both QPSK and 16-QAM. Because the PAPR is calculated by dividing the peak power in a OFDM symbol to the average power of the frame. On the other hand, the proposed method with $\lambda = 0$ increases the PAPR. The reason is that the proposed method with $\lambda = 0$ increases the power levels of the edge-most OFDM symbols so that these OFDM symbols have not the same average power. If P_{max} increases the PAPR also increases, and if D increases the PAPR decreases for the proposed method with $\lambda = 0$ as seen from the figure. Therefore, improving Doppler CRB degrades the PAPR performance unlike delay CRB as a trade-off.

VI. Conclusion

In this work, a novel constellation extension method is proposed to minimize the delay and Doppler CRBs for OFDM

DFRC systems. The proposed method improves the radar and communication performance as being transparent to the communication receiver. The proposed waveform design involves the calculation of the total number of subcarriers for power optimization, weight matrix generation for subcarrier selection, and power allocation to decrease the CRBs. In the proposed method, λ can be adjusted according to delay and Doppler accuracy requirements. The larger P_{max} values are better for the CRB minimization, but worse for average SER performance gain. Moreover, the lower D values are better for the CRB minimization, but worse for average SER performance gain. Also, the proposed method does not degrade the PAPR performance for delay CRB optimization but degrades it for Doppler CRB optimization. For the future work, the proposed method will be modified to improve the CRBs and SER performance further under the assumption of the communication channel information at the transceiver.

REFERENCES

[1] P. Yang *et al.*, "6G wireless communications: Vision and potential techniques," *IEEE Netw.*, vol. 33, no. 4, pp. 70–75, Jul. 2019.

[2] A. Yazar *et al.*, "6G vision: An ultra-flexible perspective," *ITU J. Future Evol. Technol.*, vol. 1, no. 1, pp. 121–140, Jan. 2020.

[3] W. Saad, M. Bennis, and M. Chen, "A vision of 6G wireless systems: Applications, trends, technologies, and open research problems," *IEEE Netw.*, vol. 34, no. 3, pp. 134–142, May 2019.

[4] Y. Niu, Y. Li, D. Jin, L. Su, and A. V. Vasilakos, "A survey of millimeter wave communications (mmWave) for 5G: Opportunities and challenges," *Wireless Netw.*, vol. 21, no. 8, pp. 2657–2676, 2015.

[5] F. Liu *et al.*, "Joint radar and communication design: Applications, state-of-the-art, and the road ahead," *IEEE Trans. Commun.*, vol. 68, no. 6, pp. 3834–3862, Jun. 2020.

[6] K. V. Mishra *et al.*, "Toward millimeter-wave joint radar communications: A signal processing perspective," *IEEE Signal Process. Mag.*, vol. 36, no. 5, pp. 100–114, Sep. 2019.

[7] L. Zheng, M. Lops, Y. C. Eldar, and X. Wang, "Radar and communication coexistence: An overview: A review of recent methods," *IEEE Signal Process. Mag.*, vol. 36, no. 5, pp. 85–99, Sep. 2019.

[8] A. R. Chiriyath, B. Paul, and D. W. Bliss, "Radar-communications convergence: Coexistence, cooperation, and co-design," *IEEE Trans. Cogn. Commun. Netw*, vol. 3, no. 1, pp. 1–12, Mar. 2017.

[9] M. L. Rahman *et al.*, "Framework for a perceptive mobile network using joint communication and radar sensing," *IEEE Trans. Aerosp. Electron. Syst.*, vol. 56, no. 3, pp. 1926–1941, Jun. 2019.

[10] P. Kumari *et al.*, "IEEE 802.11 ad-based radar: An approach to joint vehicular communication-radar system," *IEEE Trans. Veh. Technol.*, vol. 67, no. 4, pp. 3012–3027, Apr. 2017.

[11] H. Wymeersch *et al.*, "5G mmWave positioning for vehicular networks," *IEEE Wireless Commun.*, vol. 24, no. 6, pp. 80–86, Dec. 2017.

[12] C. B. Barneto *et al.*, "Radio-based sensing and indoor mapping with millimeter-wave 5G NR signals," in *Proc. Int. Conf. Localization GNSS (ICL-GNSS)*, Jun. 2020, pp. 1–5.

[13] ——, "Millimeter-wave mobile sensing and environment mapping: Models, algorithms and validation," *IEEE Trans. Veh. Technol.*, vol. 71, no. 4, pp. 3900–3916, Apr. 2022.

[14] E. Memisoglu, M. M. Sahin, and H. Arslan, "Orthogonal coexistence of overlapped radar and communication waveforms," in *Proc. IEEE Wireless Commun. Netw. Conf. (WCNC)*, Apr. 2022, pp. 2190–2195.

[15] M. M. Şahin and H. Arslan, "Application-based coexistence of different waveforms on non-orthogonal multiple access," *IEEE Open J. Commun. Soc*, vol. 2, pp. 67–79, 2020.

[16] J. Qian, M. Lops, L. Zheng, X. Wang, and Z. He, "Joint system design for coexistence of MIMO radar and MIMO communication," *IEEE Trans. Signal Process.*, vol. 66, no. 13, pp. 3504–3519, 2018.

[17] T. M. Schmidl and D. C. Cox, "Robust frequency and timing synchronization for OFDM," *IEEE Trans. Commun.*, vol. 45, no. 12, pp. 1613–1621, 1997.

[18] H. Minn, V. K. Bhargava, and K. B. Letaief, "A robust timing and frequency synchronization for OFDM systems," *IEEE Trans. Wireless Commun.*, vol. 2, no. 4, pp. 822–839, 2003.

[19] A. Turlapaty, Y. Jin, and Y. Xu, "Range and velocity estimation of radar targets by weighted OFDM modulation," in *Proc. IEEE Radar Conf.*, May 2014, pp. 1358–1362.

[20] D.-W. Lim, S.-J. Heo, and J.-S. No, "An overview of peak-to-average power ratio reduction schemes for OFDM signals," *J. Commun. Netw.*, vol. 11, no. 3, pp. 229–239, Jun. 2009.

[21] T. Huang and T. Zhao, "Low PMEPR OFDM radar waveform design using the iterative least squares algorithm," *IEEE Signal Process. Lett.*, vol. 22, no. 11, pp. 1975–1979, 2015.

[22] M. Bică and V. Koivunen, "Generalized multicarrier radar: Models and performance," *IEEE Trans. Signal Process.*, vol. 64, no. 17, pp. 4389–4402, 2016.

[23] C. Sturm, T. Zwick, and W. Wiesbeck, "An OFDM system concept for joint radar and communications operations," in *Proc. IEEE Veh. Technol. Conf.*, Apr. 2009, pp. 1–5.

[24] C. Sturm and W. Wiesbeck, "Waveform design and signal processing aspects for fusion of wireless communications and radar sensing," *Proc. IEEE*, vol. 99, no. 7, pp. 1236–1259, 2011.

[25] T. Guo and R. Qiu, "OFDM waveform design compromising spectral nulling, side-lobe suppression and range resolution," in *Proc. IEEE Radar Conf.*, May 2014, pp. 1424–1429.

[26] Y. Liu, G. Liao, J. Xu, Z. Yang, and Y. Zhang, "Adaptive OFDM integrated radar and communications waveform design based on information theory," *IEEE Commun. Lett*, vol. 21, no. 10, pp. 2174–2177, 2017.

[27] Z. Zhang, Z. Du, and W. Yu, "Mutual-information-based OFDM waveform design for integrated radar-communication system in Gaussian mixture clutter," *IEEE Sens. Lett.*, vol. 4, no. 1, pp. 1–4, 2019.

[28] Y. Liu, G. Liao, Z. Yang, and J. Xu, "Multiobjective optimal waveform design for OFDM integrated radar and communication systems," *Signal Process.*, vol. 141, pp. 331–342, Dec. 2017.

[29] T. Tian, G. Li, and T. Zhou, "Power distribution for an OFDM-based dual-function radar-communication sensor," *IEEE Sens. Lett.*, vol. 4, no. 11, pp. 1–4, 2020.

[30] M. Bica, K.-W. Huang, U. Mitra, and V. Koivunen, "Opportunistic radar waveform design in joint radar and cellular communication systems," in *Proc. IEEE Global Commun. Conf.*, Dec. 2015, pp. 1–7.

[31] M. Bică and V. Koivunen, "Multicarrier radar-communications waveform design for RF convergence and coexistence," in *n Proc. IEEE Int. Conf. Acoust., Speech Signal Process.*, May 2019, pp. 7780–7784.

[32] C. Shi *et al.*, "Joint subcarrier assignment and power allocation strategy for integrated radar and communications system based on power minimization," *IEEE Sensors J.*, vol. 19, no. 23, pp. 11 167–11 179, 2019.

[33] A. Ahmed, Y. D. Zhang, A. Hassanien, and B. Himed, "OFDM-based joint radar-communication system: Optimal sub-carrier allocation and power distribution by exploiting mutual information," in *Proc. Asilomar Conf. Signals Syst. Comput*, Nov. 2019, pp. 559–563.

[34] S. D. Liyanaarachchi *et al.*, "Optimized waveforms for 5G–6G communication with sensing: Theory, simulations and experiments," *IEEE Trans. Wireless Commun.*, vol. 20, no. 12, pp. 8301–8315, 2021.

[35] M. F. Keskin, V. Koivunen, and H. Wymeersch, "Limited feedforward waveform design for OFDM dual-functional radar-communications," *IEEE Trans. Signal Process.*, vol. 69, pp. 2955–2970, 2021.

[36] B. S. Krongold and D. L. Jones, "PAR reduction in OFDM via active constellation extension," *IEEE Trans. Broadcast.*, vol. 49, no. 3, pp. 258–268, 2003.

[37] C. B. Barneto *et al.*, "Full-duplex OFDM radar with LTE and 5G NR waveforms: Challenges, solutions, and measurements," *IEEE Trans. on Microw. Theory Techn.*, vol. 67, no. 10, pp. 4042–4054, Oct. 2019.

[38] M. Biedka, Y. E. Wang, Q. M. Xu, and Y. Li, "Full-duplex RF front ends: From antennas and circulators to leakage cancellation," *IEEE Microw. Mag.*, vol. 20, no. 2, pp. 44–55, Feb. 2019.

[39] L. Zheng and X. Wang, "Super-resolution delay-Doppler estimation for OFDM passive radar," *IEEE Trans. Signal Process.*, vol. 65, no. 9, pp. 2197–2210, 2017.

[40] M. Bică and V. Koivunen, "Radar waveform optimization for target parameter estimation in cooperative radar-communications systems," *IEEE Trans. . Aerosp. . Electron. Syst.*, vol. 55, no. 5, pp. 2314–2326, 2018.

[41] M. K. Simon and M.-S. Alouini, *Digital communication over fading channels*. New York: Wiley, 2001.

[42] J. R. Barry, E. A. Lee, and D. G. Messerschmitt, *Digital communication*. Springer Science & Business Media, 2012.

[43] J. G. Proakis, *Digital communications*. 4th ed. New York, NY: McGraw-Hill, 1998.